

# Acrylate Metathesis via the Second-Generation Grubbs Catalyst: Unexpected Pathways Enabled by a PCy<sub>3</sub>-Generated Enolate

Gwendolyn A. Bailey and Deryn E. Fogg\*

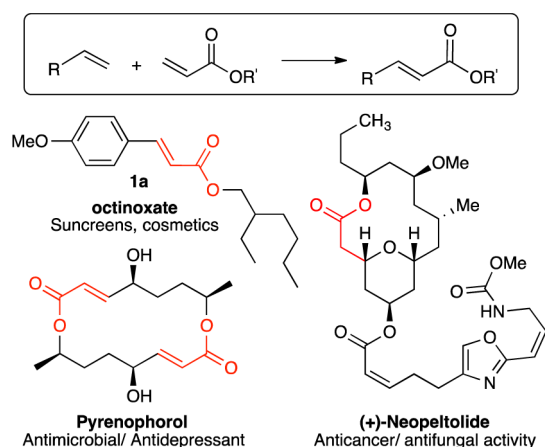
Center for Catalysis Research and Innovation and Department of Chemistry, University of Ottawa, Ottawa, Ontario K1N6N5 Canada

**S** Supporting Information

**ABSTRACT:** The diverse applications of acrylate metathesis range from synthesis of high-value  $\alpha,\beta$ -unsaturated esters to depolymerization of unsaturated polymers. Examined here are unexpected side reactions promoted by the important Grubbs catalyst **GII**. Evidence is presented for attack of PCy<sub>3</sub> on the acrylate olefin to generate a reactive carbanion, which participates in multiple pathways, including further Michael addition, proton abstraction, and catalyst deactivation. Related chemistry may be anticipated whenever labile metal–phosphine complexes are used to catalyze reactions of substrates bearing an electron-deficient olefin.

Olefin metathesis offers powerful methodologies for the synthesis of  $\alpha,\beta$ -unsaturated carbonyl compounds.<sup>1–4</sup> High-profile targets accessed via acrylate metathesis range from the high-value antioxidant **1a** to natural products of medicinal relevance (Scheme 1).<sup>5,6</sup> Cross-metathesis (CM) of acrylates

**Scheme 1. Acrylate Metathesis and Selected Products**

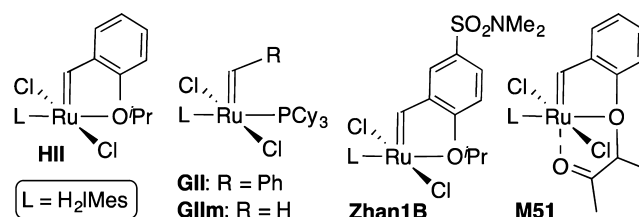


with plant-oil triglycerides or fatty acid esters is likewise key to the transformation of unsaturated fats and oils into renewable platform chemicals, including novel building blocks for high-performance surfactants.<sup>2–4,7</sup> In materials applications, related strategies have recently been deployed for depolymerization of polybutadiene<sup>8</sup> or, alternatively, assembly of bio-based polyesters<sup>9</sup> and polyamides.<sup>10–12</sup>

An influential report by Meier et al. described 50-fold higher productivity for the Hoveyda catalyst **HIII** in oleate–acrylate CM,

relative to the second-generation Grubbs catalyst **GII** (Chart 1).<sup>9,13</sup> Related catalysts (**Zhan1B**, **M51**) likewise show improved

**Chart 1. Key Catalysts Used in Acrylate Metathesis and the Resting-State Species **GII<sub>m</sub>** for the Grubbs Catalyst**



performance.<sup>14</sup> Phosphine-free catalysts are now the standard for acrylate metathesis applied to renewable feedstocks, although **GII** remains commonly used in target-directed synthesis of  $\alpha,\beta$ -unsaturated carbonyl derivatives.<sup>15</sup>

While several explanations for the superiority of phosphine-free catalysts have been advanced,<sup>16,17</sup> the mechanistic basis remains speculative. Given the large number of metathesis catalysts now based on the archetypal structures **GII** and **HIII**<sup>18</sup> and the limited understanding of the factors governing relative performance, this system affords an important target for study. Here we demonstrate that the performance of **GII** in acrylate metathesis is undermined by Michael addition pathways enabled by free PCy<sub>3</sub>, which limit yields, promote side reactions, and cause catalyst decomposition. These findings offer informed insight into catalyst choice for acrylate metathesis. In the broader context, they highlight hazards in the use of metal–phosphine complexes to promote reactions of electron-deficient olefins.

We recently noted that the excellent performance of **HIII** in acrylate–anethole metathesis is completely suppressed by added PCy<sub>3</sub> (Figure 1a).<sup>19</sup> Here we use the combination of fast-initiating **HIII** and mid-metathesis addition of PCy<sub>3</sub> to simulate highly initiated **GII**. By amplifying the concentration of the metallacyclobutane (**MCB**) intermediate relative to the off-cycle species **GII** and **GII<sub>m</sub>** which otherwise dominate, this experimental approach permits us to dissect out the impact of PCy<sub>3</sub> on the **MCB** intermediate: that is, on the active species central to the olefin metathesis reaction.

To confirm that the rapid knockdown seen in Figure 1a is due to the electron-withdrawing ester moiety, we repeated the reaction with styrene in the absence of acrylate (Figure 1b). Styrene was chosen in place of anethole to ensure formation of

Received: May 10, 2015

Published: June 1, 2015

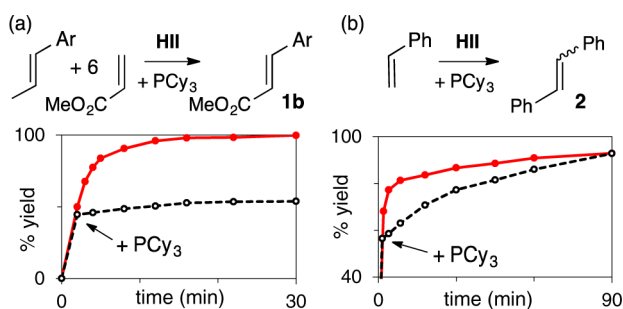


**Figure 1.** (a) Termination of CM by added PCy<sub>3</sub> in anethole–acrylate CM (Ar = 4-methoxyphenyl). (b) Rate retardation by added PCy<sub>3</sub> for CM in the absence of acrylate (0.5 mol % Ru, 70 °C, C<sub>7</sub>H<sub>8</sub>).

the key methylidene species **GII<sub>m</sub>** (the dominant species observed on treating **GII** with methyl acrylate), while subtracting ester-functionalized intermediates. In sharp contrast with the acrylate experiment, the ultimate yield of stilbene **2** was unaffected. That is, addition of PCy<sub>3</sub> merely slowed the reaction, by trapping the catalyst as the off-cycle species **GII<sub>m</sub>** and **GII** (ratio 2:3 at 0.5 h). This experiment pinpoints the acrylate ester functionality as key to the deactivating effect of PCy<sub>3</sub>, and we therefore examined the companion reaction, in which acrylate is retained but its coupling partner is omitted.

In these experiments, **HII** and PCy<sub>3</sub> were added to excess acrylate in C<sub>6</sub>D<sub>6</sub>, and the reaction was heated open to N<sub>2</sub> to permit ethylene loss.<sup>20</sup> Periodic analysis revealed formation of the phosphonium salts **A<sup>+</sup>** and **B<sup>+</sup>**, in parallel with loss of **HII** and its PCy<sub>3</sub> adduct **HII'**.<sup>21</sup> The simplicity of the <sup>31</sup>P{<sup>1</sup>H} NMR spectrum (Figure 2b) suggests that one decomposition process predominates.

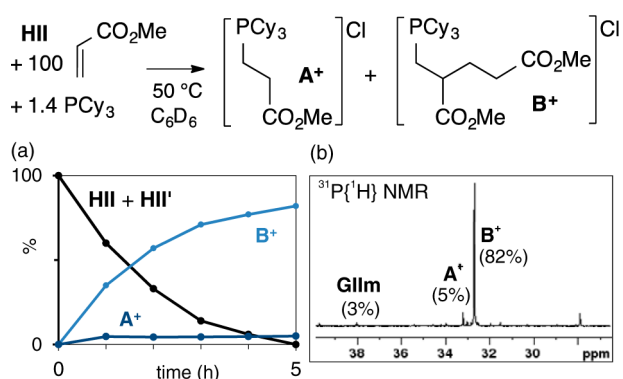
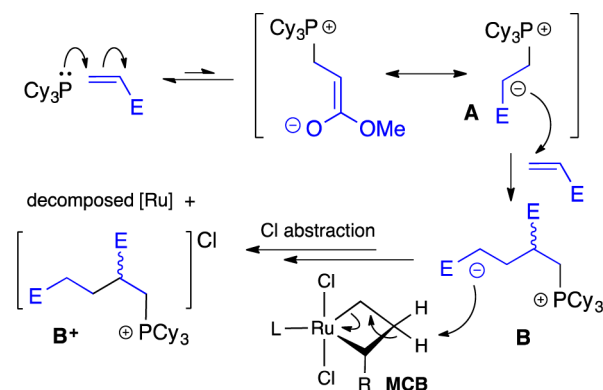


**Figure 2.** (a) Rate of loss of **HII**/**HII'** (<sup>1</sup>H NMR analysis) and formation of phosphonium salts (<sup>31</sup>P{<sup>1</sup>H} NMR analysis); curve for **GII<sub>m</sub>** omitted for clarity (<5%). (b) <sup>31</sup>P{<sup>1</sup>H} NMR spectrum of the reaction mixture at 5 h.

We propose that the phosphonium salts are generated by initial attack of PCy<sub>3</sub> on the electron-deficient olefin, forming zwitterionic **A**, which can participate in multiple subsequent pathways (Scheme 2). Ample precedent exists for this phosphonium enolate, both in phosphine-catalyzed Michael reactions<sup>22–25</sup> and in the Morita–Baylis–Hillman reaction, in which **A** participates in further nucleophilic attack on aldehyde substrates.<sup>26,27</sup>

In the present context, the dominant reaction involves attack of **A** on further acrylate, followed by proton abstraction to liberate [**B**]X. No reaction is seen in the absence of **HII**, indicating that the ruthenium species present supplies the

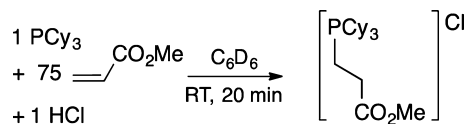
### Scheme 2. Proposed Mechanism for Acrylate-Induced Catalyst Decomposition (E = CO<sub>2</sub>Me)



required proton and counter-anion.<sup>28</sup> Chloride abstraction may provide the anion, given the absence of additional signals in NMR spectra of isolated **B<sup>+</sup>**. An **MCB** intermediate is suggested as the likely target of attack. We recently reported that **MCB** intermediates formed during styrene metathesis are rapidly deprotonated by base, including amines.<sup>29</sup> Competing attack on **GII<sub>m</sub>** is not unequivocally excluded, but is sterically less favorable.

Co-formation of **A<sup>+</sup>** indicates competing reaction of the carbon nucleophile in **A** with a proton source. **MCB** species are again candidates for attack. Adventitious water is another, and indeed the proportion of **A<sup>+</sup>** was increased on use of acrylate that was not dried over molecular sieves.<sup>30</sup> Stronger acids promote this reaction: thus, treating PCy<sub>3</sub> with methyl acrylate in the presence of HCl (Scheme 3) resulted in quantitative formation of [**A**]Cl.

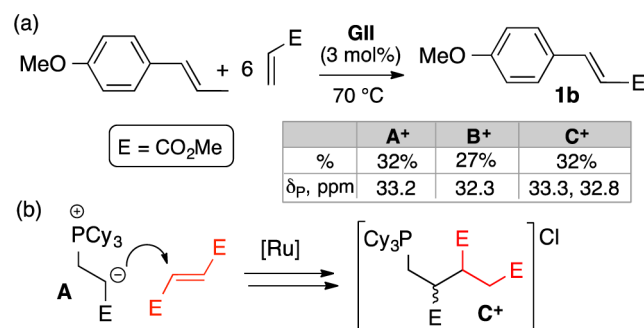
### Scheme 3. Formation of [**A**]Cl in the Presence of HCl, with No Metal Species Present



This behavior offers a new explanation for the long-established capacity of phenols to improve the productivity of the Grubbs catalysts in acrylate metathesis:<sup>31–35</sup> in short, the phenol functions as a proton source, protecting the catalyst.

The relevance of this chemistry to **GII** is supported by analysis of the anethole–acrylate CM reaction shown in Scheme 4a. Four species account for ~90% of the total <sup>31</sup>P{<sup>1</sup>H} NMR integration

### Scheme 4. (a) Decomposition of **GII** during anethole–acrylate CM. (b) Formation of **C<sup>+</sup>**



at 1 h, and for the three major ESI-MS signals. Of these species, **B**<sup>+</sup> and **A**<sup>+</sup> account for 60%. The balance is due to the new diastereomers **C**<sup>+</sup>, generated by attack of **A** on the *re* and *si* faces of methyl fumarate (Scheme 4b). Fumarate formation is due in part to the higher temperatures employed: **C**<sup>+</sup> is likewise observed at 70 °C in acrylate metathesis using the **HII**/PCy<sub>3</sub> system (16%, vs <2% at 50 °C). Also notable is the higher proportion of **A**<sup>+</sup>, which may suggest that both the **MCB** and the resting-state species **GIIm** are deprotonated by **A**. Precedents for the accessibility of the methylidene ligand of **GIIm** were noted above.

The foregoing demonstrates that the superiority of **HII** over **GII** in acrylate metathesis reactions is due to elimination of reaction pathways triggered by the ancillary PCy<sub>3</sub> ligand. The potent nucleophilicity of the latter enables efficient reaction with electron-deficient olefins, leading to unwanted byproducts and to catalyst deactivation. The well-established versatility of nucleophilic phosphines in organocatalysis points toward the broad scope of this pathway. Substrates at risk, where a phosphine ligand is liberated—whether in metathesis or other catalytic chemistry—include those bearing  $\alpha,\beta$ -unsaturated carbonyl and cyano functionalities, including acrylates, acrylamides, acrylonitriles, and  $\alpha,\beta$ -unsaturated ketones. In all of these cases, a phosphine-free catalyst is likely to offer the simplest means of achieving the desired selectivity and catalyst productivity.

## ■ ASSOCIATED CONTENT

### ■ Supporting Information

Experimental procedures and NMR spectra. The Supporting Information is available free of charge on the ACS Publications website at DOI: 10.1021/jacs.5b04524.

## ■ AUTHOR INFORMATION

### Corresponding Author

\*dfogg@uottawa.ca

### Notes

The authors declare no competing financial interest.

## ■ ACKNOWLEDGMENTS

This work was funded by NSERC of Canada. NSERC is thanked for a CGS-D fellowship to G.B. Nikita Panov is thanked for technical assistance.

## ■ REFERENCES

- (1) For recent reviews, see: (a) Prunet, J.; Grimaud, L. Cross-metathesis in Natural Products Synthesis. In *Metathesis in Natural Product Synthesis: Strategies, Substrates and Catalysts*; Cossy, J., Arseniyadis, S., Meyer, C., Eds.; Wiley-VCH: Weinheim, 2010; pp 287–312. (b) van Lierop, B. J.; Lummiss, J. A. M.; Fogg, D. E. Ring-Closing Metathesis. In *Olefin Metathesis-Theory and Practice*; Grela, K., Ed.; Wiley: Hoboken, NJ, 2014; pp 85–152. (c) Żukowska, K.; Grela, K. Cross Metathesis. In *Olefin Metathesis-Theory and Practice*; Grela, K., Ed.; Wiley: Hoboken, NJ, 2014; pp 39–84. For tandem catalysis routes to heteroaromatics, beginning with metathesis of vinyl ketones, see: (d) Donohoe, T. J.; Bower, J. F. *Proc. Natl. Acad. Sci. U.S.A.* **2010**, *107*, 3373–3376. For an analysis of the context and opportunities of these methodologies, see: (e) Krische, M. J. *Proc. Natl. Acad. Sci. U.S.A.* **2010**, *107*, 3279–3280. For a tandem intramolecular hydroarylation sequence enabled by metathesis of  $\alpha,\beta$ -unsaturated carbonyl compounds, see: (f) Chen, J.-R.; Li, C.-F.; An, X.-L.; Zhang, J.-J.; Zhu, X.-Y.; Xiao, W.-J. *Angew. Chem., Int. Ed.* **2008**, *47*, 2489–2492.
- (2) Chikkali, S.; Mecking, S. *Angew. Chem., Int. Ed.* **2012**, *51*, 5802–5808.

(3) Biermann, U.; Bornscheuer, U.; Meier, M. A. R.; Metzger, J. O.; Schäfer, H. J. *Angew. Chem., Int. Ed.* **2011**, *50*, 3854–3871.

(4) Marshall, A.-L.; Alaimo, P. J. *Chem.—Eur. J.* **2010**, *16*, 4970–4980.

(5) Lummiss, J. A. M.; Oliveira, K. C.; Pranckevicius, A.; Santos, A.; dos Santos, E. N.; Fogg, D. E. *J. Am. Chem. Soc.* **2012**, *134*, 18889–18891.

(6) For recent applications in the synthesis of natural products of medicinal relevance, see: (a) Plummer, C. W.; Wei, C. S.; Yozwiak, C. E.; Soheili, A.; Smithback, S. O.; Leighton, J. L. *J. Am. Chem. Soc.* **2014**, *136*, 9878–9881. (b) Chatterjee, S.; Ghadigaonkar, S.; Sur, P.; Sharma, A.; Chattopadhyay, S. *J. Org. Chem.* **2014**, *79*, 8067–8076. (c) Xiao, Q.; Jackson, J. J.; Basak, A.; Bowler, J. M.; Miller, B. G.; Zakarian, A. *Nat. Chem.* **2013**, *5*, 410–416. (d) Willwacher, J.; Fürstner, A. *Angew. Chem., Int. Ed.* **2014**, *53*, 4217–4221. (e) Fuwa, H.; Saito, A.; Sasaki, M. *Angew. Chem., Int. Ed.* **2010**, *49*, 3041–3044. (f) Brewitz, L.; Llaviera, J.; Yada, A.; Fürstner, A. *Chem.—Eur. J.* **2013**, *19*, 4532–4537.

(7) Corma, A.; Iborra, S.; Velty, A. *Chem. Rev.* **2007**, *107*, 2411–2502.

(8) Schulz, M. D.; Ford, R. R.; Wagener, K. B. *Polym. Chem.* **2013**, *4*, 3656–3658.

(9) Rybak, A.; Meier, M. A. R. *Green Chem.* **2007**, *9*, 1356–1361.

(10) Miao, X.; Fischmeister, C.; Dixneuf, P. H.; Bruneau, C.; Dubois, J. L.; Couturier, J. L. *Green Chem.* **2012**, *14*, 2179–2183.

(11) Malacea, R.; Fischmeister, C.; Bruneau, C.; Dubois, J.-L.; Couturier, J.-L.; Dixneuf, P. H. *Green Chem.* **2009**, *11*, 152–155.

(12) Winkler, M.; Meier, M. A. R. *Green Chem.* **2014**, *16*, 3335–3340.

(13) The superior performance of **HII** relative to **GII** for acrylate metathesis has since been confirmed in multiple reports; see refs 8, 10, and: (a) Schweitzer, D.; Snell, K. D. *Org. Process Res. Dev.* **2015**, advance article. DOI: 10.1021/op5003006. (b) Lafaye, K.; Nicolas, L.; Guérinot, A.; Reymond, S. b.; Cossy, J. *Org. Lett.* **2014**, *16*, 4972–4975. (c) Meng, X.; Matson, J. B.; Edgar, K. J. *Biomacromolecules* **2014**, *15*, 177–187. (d) Bilel, H.; Hamdi, N.; Zagrouba, F.; Fischmeister, C.; Bruneau, C. *Green Chem.* **2011**, *13*, 1448–1452. (e) Djigoué, G. B.; Meier, M. A. R. *Appl. Catal., A* **2009**, *368*, 158–162.

(14) See refs 10, 13a, d, e, and: (a) Vignon, P.; Vancompernelle, T.; Couturier, J.-L.; Dubois, J.-L.; Mortreux; Gauvin, R. M. *ChemSusChem* **2015**, *8*, 1143–1146. (b) Ho, T. T.; Jacobs, T.; Meier, M. A. R. *ChemSusChem* **2009**, *2*, 749–754.

(15) For selected noteworthy examples, see refs 1a, 6e, and: (a) Cash, B. M.; Prevost, N.; Wagner, F. F.; Comins, D. L. *J. Org. Chem.* **2014**, *79*, 5740–5745. (b) Kinzurik, M. I.; Hristov, L. V.; Matsuda, S. P. T.; Ball, Z. T. *Org. Lett.* **2014**, *16*, 2188–2191. (c) Beemelmans, C.; Gross, S.; Reissig, H.-U. *Chem.—Eur. J.* **2013**, *19*, 17801–17808. (d) Trost, B. M.; Aponick, A.; Stanzl, B. N. *Chem.—Eur. J.* **2007**, *13*, 9547–9560. (e) Marjanovic, J.; Kozmin, S. A. *Angew. Chem., Int. Ed.* **2007**, *46*, 8854–8857. Additional examples appear in a recent review of RCMT methods for the synthesis of lactones from acrylates; see: (f) Bassetti, M. D. A.; Andrea. *Curr. Org. Chem.* **2013**, *17*, 2654–2677.

(16) Early suggestions centered on the limited capacity of the electron-deficient olefin to compete with PCy<sub>3</sub> for binding to the metal; see: (a) Love, J. A.; Morgan, J. P.; Trnka, T. M.; Grubbs, R. H. *Angew. Chem., Int. Ed.* **2002**, *41*, 4035–4037. (b) Hoveyda, A. H.; Gillingham, D. G.; Van Veldhuizen, J. J.; Kataoka, O.; Garber, S. B.; Kingsbury, J. S.; Harrity, J. P. A. *Org. Biomol. Chem.* **2004**, *2*, 8–23 Conversely, excessively strong binding of PCy<sub>3</sub> to electron-deficient Ru intermediates has been proposed: see ref 16(b).

(17) Also potentially plausible is nucleophilic attack of PCy<sub>3</sub> on the electron-deficient alkylidene, by analogy to the pathway established for the methylidene complexes RuCl<sub>2</sub>(L)(PCy<sub>3</sub>)(=CH<sub>2</sub>). Crystallographic evidence demonstrating attack of PCy<sub>3</sub> on the methylidene ligand was recently reported; see: (a) Lummiss, J. A. M.; McClennan, W. L.; McDonald, R.; Fogg, D. E. *Organometallics* **2014**, *33*, 6738–6741. Abstraction of the methylidene moiety from isolated **GIIm** liberates [MePCy<sub>3</sub>]Cl; see: (b) Hong, S. H.; Wenzel, A. G.; Salguero, T. T.; Day, M. W.; Grubbs, R. H. *J. Am. Chem. Soc.* **2007**, *129*, 7961–7968. For evidence of this pathway during catalysis, see: (c) Lummiss, J. A. M.; Ireland, B. J.; Sommers, J. M.; Fogg, D. E. *ChemCatChem* **2014**, *6*, 459–463. While nucleophilic attack of phosphine on Ru-alkylidene species is rare, Diver has demonstrated such a pathway where CO binding rendered the alkylidene carbon more electrophilic; see: Galan, B. R.;

Pitak, M.; Keister, J. B.; Diver, S. T. *Organometallics* **2008**, *27*, 3630–3632.

(18) (a) Vougioukalakis, G. C. Ruthenium-Benzylidene Olefin Metathesis Catalysts. In *Olefin Metathesis-Theory and Practice*; Grela, K., Ed.; Wiley: Hoboken, NJ, 2014; pp 397–416. (b) Ginzburg, Y.; Lemcoff, N. G. Hoveyda-Type Olefin Metathesis Complexes. In *Olefin Metathesis-Theory and Practice*; Grela, K., Ed.; Wiley: Hoboken, NJ, 2014; pp 437–451.

(19) Bates, J. M.; Lummiss, J. A. M.; Bailey, G. A.; Fogg, D. E. *ACS Catal.* **2014**, *4*, 2387–2394.

(20) These experiments were carried out at 50 °C, to permit interception of low-energy organometallic pathways, rather than downstream events. At higher temperatures, attack of **A** on additional CM products is observed; see text.

(21) The cation **B**<sup>+</sup> was identified by mass spectrometric and NMR analysis of material isolated by aqueous extraction. The cation is unperturbed by isolation, as confirmed by spiking a reaction aliquot with the isolated salt and assessing the <sup>31</sup>P{<sup>1</sup>H} NMR spectrum. Diagnostic for the structure of **B**<sup>+</sup> is the upfield location and doublet multiplicity of the <sup>13</sup>C{<sup>1</sup>H} NMR signal for PCH<sub>2</sub> (C5:17.5 ppm, d, <sup>1</sup>J<sub>PC</sub> = 44 Hz; see SI). This signal exhibits the expected HMQC correlation to two diastereotopic methylene protons (δ 2.84, ddd, *J*<sub>HH</sub> = 16 Hz, <sup>2</sup>J<sub>PH</sub> = 12 Hz, *J*<sub>HH</sub> = 10 Hz, 1H; δ 2.35, m, 1H). The <sup>13</sup>C{<sup>1</sup>H} NMR doublet at 38.2 for the PCH<sub>2</sub>CH methine carbon also exhibits the expected HMBC correlations with the adjacent methylene protons (H5, H9, and H10); see SI.

(22) Fan, Y. C.; Kwon, O. *Chem. Commun.* **2013**, *49*, 11588–11619.

(23) Methot, J. L.; Roush, W. R. *Adv. Synth. Catal.* **2004**, *346*, 1035–1050.

(24) Gimbert, C.; Lumbierres, M.; Marchi, C.; Moreno-Mañas, M.; Sebastián, R. M.; Vallribera, A. *Tetrahedron* **2005**, *61*, 8598–8605.

(25) Gómez-Bengoa, E.; Cuerva, J. M.; Mateo, C.; Echavarren, A. M. *J. Am. Chem. Soc.* **1996**, *118*, 8553–8565.

(26) Morita, K.-I.; Suzuki, Z.; Hirose, H. *Bull. Chem. Soc. Jpn.* **1968**, *41*, 2815–2815.

(27) Basavaiah, D.; Rao, A. J.; Satyanarayana, T. *Chem. Rev.* **2003**, *103*, 811–892.

(28) The Ru center may also act as a Lewis acid, complexing the carbonyl group of **A**, and thus favoring subsequent Michael addition reactions. Such behaviour was reported for a related Ru–hydride complex; see ref 25.

(29) Ireland, B. J.; Dobbigny, B. T.; Fogg, D. E. *ACS Catal.* **2015**, submitted.

(30) The phenol inhibitors present in methyl acrylate are not significant contributors. The maximum level of 100 ppm 4-methoxyphenol cited in the supplier's specification sheet (Sigma-Aldrich; 99% purity reagent) would account for just 0.5% yield of **A**<sup>+</sup>.

(31) Adding a phenol (the renewable phenol guaiacol) to the reaction resulted in selective formation of [**A**]Cl; see SI.

(32) Forman, G. S.; Tooze, R. P. *J. Organomet. Chem.* **2005**, *690*, 5863–5866.

(33) Forman, G. S.; McConnell, A. E.; Tooze, R. P.; Van Rensburg, W. J.; Meyer, W. H.; Kirk, M. M.; Dwyer, C. L.; Serfontein, D. W. *Organometallics* **2005**, *24*, 4528–4542.

(34) Schmidt, B.; Hauke, S. *Org. Biomol. Chem.* **2013**, *11*, 4194–4206.

(35) Scavenging of phosphine offers an alternative solution. CuI has recently been employed to enhance yields in **GII**-promoted acrylate metathesis; see: (a) Nair, R. N.; Bannister, T. D. *J. Org. Chem.* **2014**, *79*, 1467–1472. (b) Voigtritter, K.; Ghorai, S.; Lipshutz, B. H. *J. Org. Chem.* **2011**, *76*, 4697–4702. As expected, adding CuI during the anethole–acrylate CM reaction completely suppressed formation of the phosphonium salts. Instead visible in the <sup>31</sup>P{<sup>1</sup>H} NMR spectrum were a sharp singlet for [MePCy<sub>3</sub>]Cl (34.0 ppm) and a broad singlet at 12.89 ppm, likely corresponding to a copper-phosphine adduct.